

# A Bio-Inspired Support of Gold Nanoparticles–Chitosan Nanocomposites Gel for Immobilization and Electrochemical Study of K562 Leukemia Cells

Lin Ding, Chen Hao, Yadong Xue, and Huangxian Ju\*

Key Laboratory of Analytical Chemistry for Life Science (Education Ministry of China), Department of Chemistry, Nanjing University, Nanjing 210093, China

Received December 26, 2006; Revised Manuscript Received February 3, 2007

A novel nanocomposites gel was prepared by neutralizing a designer nanocomposites solution of chitosan encapsulated gold nanoparticles formed by reducing in situ tetrachloroauric acid in chitosan. The bio-inspired gel was designed for immobilization and electrochemical study of cells and monitoring adhesion, proliferation, and apoptosis of cells on electrodes. Using K562 leukemia cells as a model, an impedance cell sensor was constructed. The methods for preparation of the gel and immobilization of cells were simple and “green”. The nanocomposites gel showed improved immobilization capacity for cells and good biocompatibility for preserving the activity of immobilized living cells. The living cells immobilized on glassy carbon electrode exhibited an irreversible voltammetric response and increased the electron-transfer resistance with a good correlation to the logarithmic value of concentration ranging from  $1.34 \times 10^4$  to  $1.34 \times 10^8$  cells  $\text{mL}^{-1}$  with a limit of detection of  $8.71 \times 10^2$  cells  $\text{mL}^{-1}$  at  $10\sigma$ . This work implied that the nanocomposites gel based on biopolymer and nanoparticles possessed potential applications for biosensing and provided a new avenue for electrochemical investigation of cell adhesion, proliferation, and apoptosis.

## Introduction

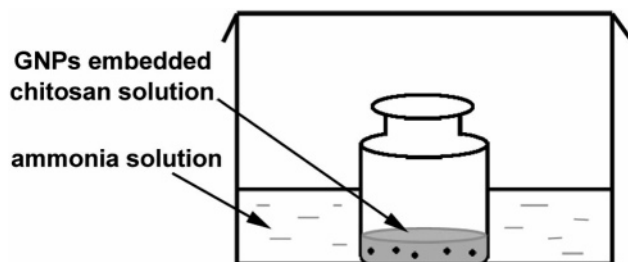
Over the past decade, significant progress has been made in building toolboxes for investigation of immobilized whole cells. Simple and nondestructive electrochemical methods have attracted considerable attention for studying efficiently intact living cells,<sup>1</sup> constructing electrical impedance-based sensing system to track the morphological change of adherent cells,<sup>2</sup> and monitoring cell response to drugs.<sup>3</sup> To reap the full potential offered by these methods, simultaneous control of electronic and cell immobilization properties at the cell/electrode interface is of vital importance. Despite extensive effort launched in this area, the construction of an interface that fulfills both requirements, however, remains a challenging task.

With unique chemical and physical properties, gold nanoparticles (GNPs) have shown widespread use in fundamental research,<sup>1,4–6</sup> particularly in biological<sup>5</sup> and sensing applications.<sup>6</sup> Incorporation of GNPs into polymer matrices has attracted increasing interest in improving the stability and biocompatibility of GNPs and enhancing their capability for immobilization due to the superior properties of the formed nanocomposites to both the polymer matrices and the nanoparticles.<sup>7</sup> Ideally, this polymeric material should be biocompatible and have reactive functional groups for further attachment of biomolecules.<sup>8</sup> One such natural polymer is chitosan that offers distinctive advantages such as good biocompatibility, nontoxicity, remarkable affinity to proteins, and excellent gel-forming ability.<sup>9,10</sup> Chitosan-based materials have been extensively applied as immobilization matrices for preparation of biosensors.<sup>11–15</sup> To the best of our knowledge, no work focused on the synthesis of GNPs-embedded chitosan nanocomposites gel (GNPs–CHIT gel) has been reported except several solutions of gold<sup>16–18</sup> or

platinum nanoparticle-doped chitosan.<sup>12</sup> In the present work, GNPs were produced in situ in chitosan solution, and the resultant homogeneous GNPs–chitosan nanocomposites solution could be readily made into nanocomposites gel. The whole process did not introduce any environmental toxicity or biological hazards according to the 12 fundamental principles of green chemistry, and was thus green.<sup>19</sup> The GNPs embedded in the three-dimensional chitosan network could serve as electron conductor. The designer nanocomposite system combined the unique properties of chitosan and GNPs, and thus could provide a nontoxic support for cells to efficiently retain their good activity and an opportunity for construction of a sensitive impedance cell sensor, which was based on the change of the electron-transfer impedance of redox probe upon K562 cells immobilization, adhesion, and proliferation on the support.

Electrochemical impedance spectroscopy (EIS) is an alternative powerful tool for monitoring the changes of interfacial properties at electrode surfaces.<sup>20</sup> This technique has been used for interaction detection between biomolecules and cells<sup>21</sup> and development of cell sensors.<sup>22–25</sup> A Faradaic impedance-based cell sensor has been prepared by immobilizing *E. coli* O157: H7 on an indium–tin oxide interdigitated array microelectrode, which shows a linear relationship between the electron-transfer resistance of one redox probe and logarithm of the cell concentration ranging from  $4.36 \times 10^5$  to  $4.36 \times 10^8$  cfu  $\text{mL}^{-1}$ .<sup>22</sup> In comparison with surface plasmon resonance and quartz crystal microbalance techniques, which are also used for interaction study between biomolecules or biomolecules and cells, the EIS technique is low-cost and relatively easy to use. Here, the designer bio-inspired gel was proposed for the development of a novel impedance sensor for tumor cells. The sensor showed a correlation between the electron-transfer resistance of one redox probe at the electrode and the concentration of K562 cells. The immobilized cells showed sensitive voltammetric response and good activity of living cells, sug-

\* Corresponding author. Phone: +86-25-83593593. Fax: +86-25-83593593. E-mail: hxju@nju.edu.cn.

**Scheme 1.** Experimental Setup for Sol–Gel Transition of GNPs–CHIT Solution in a Gaseous Ammonia Atmosphere

gesting a potential application of nanocomposite material in electrochemical sensing for monitoring the adhesion, electrochemical behaviors, viability, proliferation, and apoptosis of living cells.

### Experimental Section

**Materials.**  $\text{AuCl}_3\text{HCl}\cdot 4\text{H}_2\text{O}$  ( $\text{Au\%} > 48\%$ ) and chitosan ( $\text{MW } (1.9\text{--}3.1) \times 10^5$ ; 85–90% deacetylation) were obtained from Aldrich (USA). Phosphate buffer saline (PBS) ( $\text{pH } 7.4$ ) containing  $\text{NaCl } 137 \text{ mM}$ ,  $\text{KCl } 2.7 \text{ mM}$ ,  $\text{Na}_2\text{HPO}_4\cdot 12\text{H}_2\text{O } 87.2 \text{ mM}$ , and  $\text{KH}_2\text{PO}_4$   $14.1 \text{ mM}$  was used as electrolyte. Potassium ferrocyanide and potassium ferricyanide were purchased from Shanghai Chemical Reagent Co., Ltd. (China). The solutions were prepared with deionized water of  $18 \text{ M}\Omega$  purified from a Milli-Q purification system.

**Cell Line and Cell Culture.** K562 cell line was kindly provided by the Affiliated Zhongda Hospital, Southeast University, Nanjing, China. K562 cells were cultured in a flask in RPMI 1640 medium (GIBCO) supplemented with 10% fetal calf serum (FCS, Sigma), penicillin ( $100 \mu\text{g mL}^{-1}$ ), and streptomycin ( $100 \mu\text{g mL}^{-1}$ ) at  $37^\circ\text{C}$  in a humidified atmosphere containing 5%  $\text{CO}_2$ . After 72 h, the cells were collected and separated from the medium by centrifugation at  $1000 g$  for 10 min, and then washed twice with a sterile  $\text{pH } 7.4$  PBS. The sediment was resuspended in the PBS to obtain a homogeneous cell suspension. Cell number was determined using a Petroff-Hausser cell counter (USA).

**Preparation of Gold Nanoparticles-Embedded Chitosan Nanocomposites Sol.** Gold nanoparticles were prepared using chitosan as reducing/stabilizing reagent according to a modified method.<sup>16</sup> All glassware was cleaned in a bath of freshly prepared aqua regia solution ( $\text{HCl}:\text{HNO}_3$  3:1) and then rinsed thoroughly with  $\text{H}_2\text{O}$  prior to use. Prior to the preparation of GNPs, 1% chitosan solution was prepared by dissolving a certain amount of chitosan in 1% acetic acid. Because of the poor solubility of chitosan, the mixture was first vortexed and then filtered through  $0.22\text{-}\mu\text{m}$  Millipore syringe filters to remove any impurities.  $1.32 \text{ mL}$  of a  $0.33\%$   $\text{HAuCl}_4$  solution was added dropwise to  $10 \text{ mL}$  of a solution of 1% chitosan under magnetic stirring, and then the mixture was heated to  $80^\circ\text{C}$  using a water bath and allowed to stay for 2 h, at which a red GNPs–CHIT solution was obtained.

To prepare the GNPs-embedded chitosan nanocomposites gel (GNPs–CHIT gel), a vial containing  $0.25 \text{ mL}$  of resultant GNPs–CHIT solution diluted with  $2.25 \text{ mL}$  of 1% chitosan solution was placed in a glass reactor containing  $20 \text{ mL}$  of 1% ammonia solution (Scheme 1). The sample was allowed to stand for 24 h in the reactor. The obtained GNPs–CHIT sol was then taken out of the vial and dialyzed to remove ammonium acetate. The concentration of GNPs in the sol was  $18.6 \mu\text{g mL}^{-1}$ .

**Electrode Modification with GNPs–CHIT Gel and Cell Immobilization.** The glassy carbon electrode (GCE) was first polished with  $1.0$ ,  $0.3$ , and  $0.05 \mu\text{m}$   $\alpha\text{-Al}_2\text{O}_3$  powder (Beuhler) successively and rinsed thoroughly with deionized water.  $5 \mu\text{L}$  of GNPs–CHIT sol was then dropped onto the GCE to form a nanocomposites gel film (GNPs–CHIT gel/GCE). Following a rinse with deionized water, the electrode was immersed in a suspension of  $2.0 \times 10^6 \text{ cell mL}^{-1}$  for 1 h to achieve

cell immobilization. The K562 cells immobilized GNPs–CHIT gel/GCE (cells/GNPs–CHIT gel/GCE) was washed thoroughly with deionized water and used for electrochemical measurements. As a control, three films were prepared on GCE by dropping  $5 \mu\text{L}$  of CHIT solution, GNPs–CHIT solution, and CHIT sol on the electrodes, respectively. The CHIT sol was synthesized by the same procedure as shown in Scheme 1.

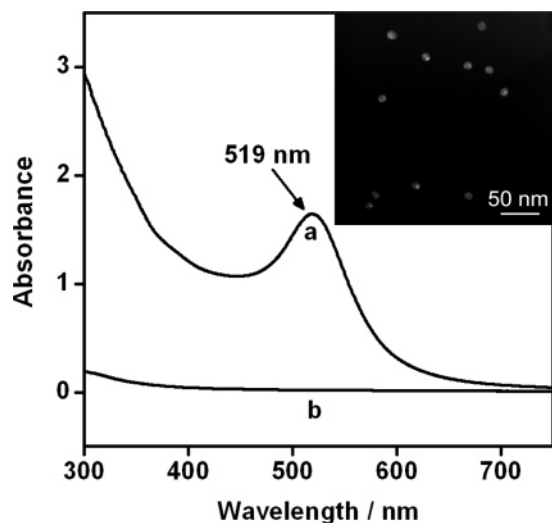
**Cell Proliferation on GNPs–CHIT Gel Film.**  $10 \mu\text{L}$  of  $2.0 \times 10^5 \text{ cells mL}^{-1}$  K562 cells was introduced onto the GNPs–CHIT gel film, which was coated on glassy dishes, and cultured in RPMI 1640 medium (GIBCO, Grand Island, NY) supplemented with 10% FCS, penicillin ( $100 \mu\text{g mL}^{-1}$ ), and streptomycin ( $100 \mu\text{g mL}^{-1}$ ) at  $37^\circ\text{C}$  in a humidified atmosphere containing 5%  $\text{CO}_2$ . After the adhered K562 cells were cultured for successively different periods, the photos of K562 cells proliferated on the nanocomposites film were recorded on an optical microscope (DMLP, Leica) with a magnification of  $200\times$ , provided with a camera. For electrochemically monitoring cell adhesion and proliferation, the GNPs–CHIT gel film was coated on GCE before cells were introduced, and the impedance measurements were carried out on a PGSTAT30/FRA2 system (Autolab, Netherlands); other culture conditions were the same as those used for optical observation.

**Apparatus and Characterizations.** The UV–vis properties of the GNPs–CHIT solution were characterized with a UV-2401 spectrophotometer (Shimadzu, Kyoto, Japan). The morphology of GNPs in the prepared nanocomposites was observed under a JEM-200CX transmission electron microscope (TEM, JEOL, Japan) operating at  $200 \text{ kV}$  on a  $400$  mesh carbon-coated copper grid. Fourier-transform infrared spectroscopy (FTIR) was carried out on a NEXUS 870 FTIR (Nicolet, USA) equipped with an omni sampler over 32 scans. The samples of CHIT, GNPs–CHIT, and GNPs–CHIT sol were prepared by drop coat and droplet evaporation of these solutions on KBr tablets, respectively. After  $10 \mu\text{L}$  of CHIT solution, GNPs–CHIT solution, and GNPs–CHIT sol was dropped on cover slips, the morphologies of dried films were observed under a 1530VP scanning electron microscope (SEM, LEO, Germany).

**Electrochemical Measurements.** Cyclic voltammetric measurements were performed on a CHI 730 electrochemical analyzer (CH Instruments, Inc.) in  $\text{pH } 7.4$  PBS using a conventional three-electrode system with modified GCE as working, platinum wire as auxiliary, and saturated calomel electrode as reference electrodes. EIS measurements were carried out on a PGSTAT30/FRA2 system (Autolab, Netherlands) using the three-electrode setup in  $0.01 \text{ M pH } 7.4$  PBS containing  $10 \text{ mM Fe}(\text{CN})_6^{3-/4-}$  and  $0.1 \text{ M KCl}$ . The impedance spectra were recorded within the frequency range of  $10^{-2}$ – $10^6 \text{ Hz}$ . The amplitude of the applied sine wave potential in each case was  $5 \text{ mV}$ . All of the experiments were performed at  $37 \pm 0.5^\circ\text{C}$ .

### Results and Discussion

**Characterization of GNPs–CHIT Nanocomposites Solution.** The preparation of a homogeneous solution of GNPs–CHIT nanocomposites was a key step in this work. The deep red-colored solution of CHIT-capped GNPs obtained with a one-pot strategy exhibited a UV–vis absorption peak centered at  $519 \text{ nm}$  (Figure 1a), a typical surface plasmon resonance band for GNPs,<sup>16</sup> while no absorption was observable for chitosan solution (Figure 1b), indicating the formation of GNPs. The surface plasmon absorption has been proven very sensitive to the size, shape, and spatial distribution of metallic nanoparticles, and the increase in the size can cause a red shift of the absorption peak.<sup>17,26</sup> For example, two kinds of GNPs reported with the sizes of  $10$  and  $24 \text{ nm}$  showed the absorption peaks at  $524^{26}$  and  $530^{27} \text{ nm}$ , respectively. The sharp UV–vis absorption peak indicated the size distribution of the obtained GNPs was uniform. The TEM photo of the GNPs showed uniform spherical shape and monodispersion with a diameter of  $12 \text{ nm}$  (inset,



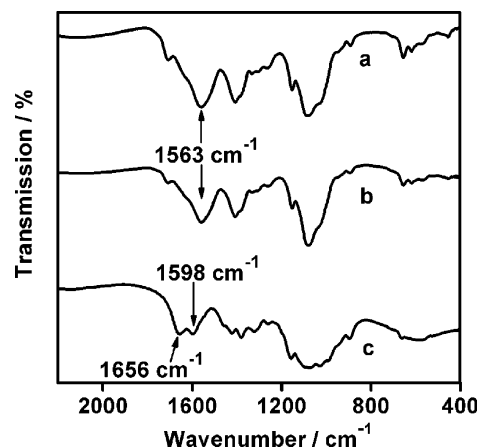
**Figure 1.** UV-vis absorption spectra of (a) GNPs obtained in 1% chitosan + 1% HAc, and (b) 1% chitosan + 1% HAc solution. Inset: TEM image of the obtained GNPs.

Figure 1). The larger size of the obtained GNPs showed lower plasmon absorption wavelength than that reported by Huang et al.,<sup>26</sup> indicating different media surrounding the nanoparticles. This appearance implied that the GNPs were surrounded by chitosan to form GNPs-CHIT nanocomposites due to the electrostatic attraction between protonized amino group of chitosan and negatively charged GNPs. This was proven by decreasing the acidity of GNPs-CHIT nanocomposites solution. After NaOH was added to the solution, red sediment was observed. The surrounding of chitosan around nanoparticles stabilized GNPs. No aggregation could be identified by TEM, even after 2 months.

**Preparation and Characterization of GNPs-CHIT Nanocomposites Gel.** An ammonia technique, originally developed for the formation of genuine chitosan physical hydrogel,<sup>28</sup> was used to prepare GNPs-CHIT nanocomposites sol by simply putting the GNPs-CHIT solution in contact with gaseous ammonia as a neutralization reagent to induce the formation of sol. The sol formation process could be roughly divided into two stages: initially, gaseous ammonia diffused in the acidic nanocomposites solution and neutralized the  $H^+$ ; second, with the increasing pH the charge density of chitosan decreased, which made the polymer chains more flexible. This allowed the occurrence of chain entanglement and generation of physical junctions, which ultimately led to the formation of an extensive polymer network and the GNPs-CHIT nanocomposites sol.<sup>28</sup>

Evidence for the neutralization of  $-NH_3^+$  could be observed from an IR spectroscopic measurement. The films prepared with both chitosan and GNPs-CHIT solutions showed the strong absorption of  $-NH_3^+$  deformation at  $1563\text{ cm}^{-1}$ <sup>29</sup> (Figure 2a and b), which covered the characteristic absorption of amide I ( $C=O$  in  $O=C-NH$ ) and amide II ( $-NH$  in  $O=C-NH$ ) of CHIT. With the gradual neutralization of  $-NH_3^+$ , the strong adsorption at  $1563\text{ cm}^{-1}$  disappeared; thus the peaks at  $1656$  and  $1598\text{ cm}^{-1}$  for amide I and amide II of CHIT<sup>30</sup> could be observed (Figure 2c), which verified the formation of the nanocomposites sol.

The SEM images showed a polymer network of the gel different from those of other films (Figure 3). The GNPs-CHIT gel film was comprised of nanometer-scaled spheres that were aggregated to form a rough, porous surface, attributable to the formation of polymer network accompanying the neutralization, while the films prepared with chitosan and GNPs-CHIT



**Figure 2.** Comparison of FTIR transmission spectra of chitosan solution (a), GNPs-CHIT solution (b), and GNPs-CHIT sol (c).

solutions exhibited smaller particles with flat and featureless morphology. The gold particles were embedded in the chitosan matrix; thus they could not be observed. One critical parameter for immobilization of cells is the roughness of the surface.<sup>31</sup> In comparison with the other two films, the rough surface of the GNPs-CHIT gel film could serve as a better medium for cell immobilization. Moreover, the porous property of the nanocomposite on the electrode made the redox probe more accessible to the electrode surface, thus facilitating the electron transfer.

**Cyclic Voltammetric Behavior of K562 Cells on Nanocomposites-Modified Electrode.** A living cell can be properly described as an electrochemical dynamic system.<sup>32,33</sup> Figure 4A shows the electrochemical behavior of living cells immobilized on GNPs-CHIT gel-modified electrode. An irreversible oxidation peak was identified at  $+0.76\text{ V}$  on cells/GNPs-CHIT gel/GCE, while no peak was observable on both bare and GNPs-CHIT gel-modified GCE. The irreversible oxidation peak disappeared in the second scan (not shown). The background current of the GNPs-CHIT gel/GCE (b) was greater than that of bare GCE (a), likely due to the resistance and double layer capacitance caused by chitosan. The electrochemical response of the immobilized living cells was attributed to the conversion of guanine in cell cytoplasm to 8-oxo-guanine.<sup>3</sup> Considering the irreversibility of the electrode process of K562 cells and the decrease of peak current upon continuous cyclic sweep, the peak current from the first scan was applicable to the characterization of cell viability.

As the control, the voltammetric responses were also monitored for K562 cells adsorbed on chitosan, GNPs-CHIT, and chitosan gel-modified GCE with the same cell immobilization process (Figure 4B). All three electrodes showed poor responses of the living cells. Both the presence of GNPs and the formation of gel could improve the oxidation process to move the oxidation peak from  $+0.90$  to  $+0.81\text{ V}$  (curves b and c, Figure 4B), attributable to the poor electrical conductivity of chitosan film, the presence of GNPs, and good spatial structure of the gel support. GNPs could effectively promote electron transfer between cells and GCE and facilitate the exposure of functional groups on cell surfaces.<sup>1</sup> The GNPs without CHIT, produced by sodium citrate reduction approach, were also applied to modify GCE for examining the influence of CHIT on cell immobilization. Different from the GNPs-modified carbon paste electrode,<sup>1</sup> it was impossible to prepare a stable gold nanoparticles-modified GCE for adhesion of cells without the presence of chitosan. The gel formation led to a surface with desired roughness and porosity that was ideal for cell immobilization



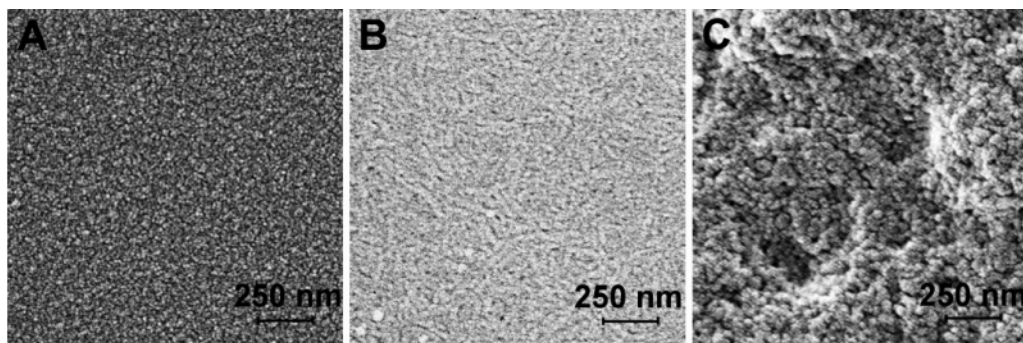


**Figure 3.** SEM images of films prepared from CHIT solution (A), GNPs-CHIT solution (B), and GNPs-CHIT gel (C).

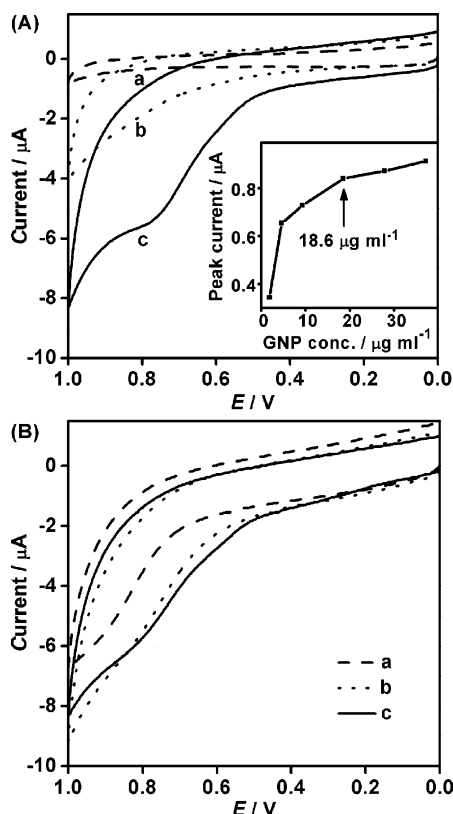


**Figure 4.** Cyclic voltammograms of bare GCE (a), GNPs-CHIT gel/GCE (b), and cells/GNPs-CHIT gel/GCE (c) (A); and chitosan (a), and CHIT gel (c) films after immersion in  $2 \times 10^6$  cells  $\text{mL}^{-1}$  K562 cells suspension for 1 h (B) in pH 7.4 PBS. Scan rate:  $50 \text{ mV s}^{-1}$ . Inset in (A): effect of GNPs concentration in gel on peak current of cells/GNPs-CHIT gel/GCE.

and electron transfer. Therefore, GNPs-CHIT gel used as immobilization matrix possessed the excellent properties offered by both GNPs and the spatial structure of the polymer gel network.

To further evaluate the effect of GNPs, an investigation was carried out to relate the dependence of anodic peak current of cells/GNPs-CHIT gel/GCE on the amount of GNPs in gel (Figure 4A, inset). With the increasing amount of GNPs, the response increased and trended to a maximum value at  $18.6 \mu\text{g mL}^{-1}$ . Overhigh GNPs concentration would lead to the instability of the response and leakage of GNPs out of the film. Thus, the GNPs-CHIT solution containing  $18.6 \mu\text{g mL}^{-1}$  GNPs was used for the preparation of GNPs-CHIT gel/GCE.

#### Transduction Principle of Cell-Based Impedance Sensor.

The cell-based sensor was based on the measurement of electron-transfer resistance ( $R_{\text{et}}$ ) with  $[\text{Fe}(\text{CN})_6]^{3-/4-}$  as a redox probe. The  $R_{\text{et}}$  values were measured three times from the

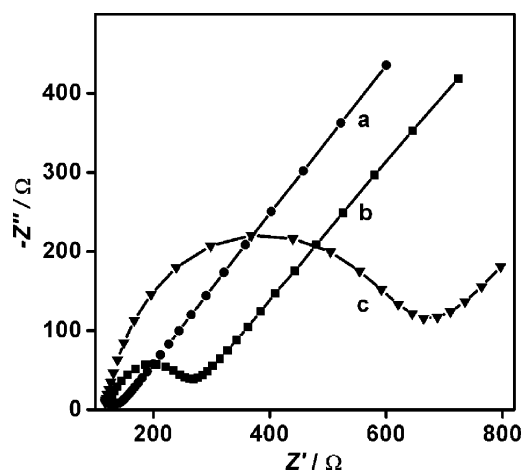
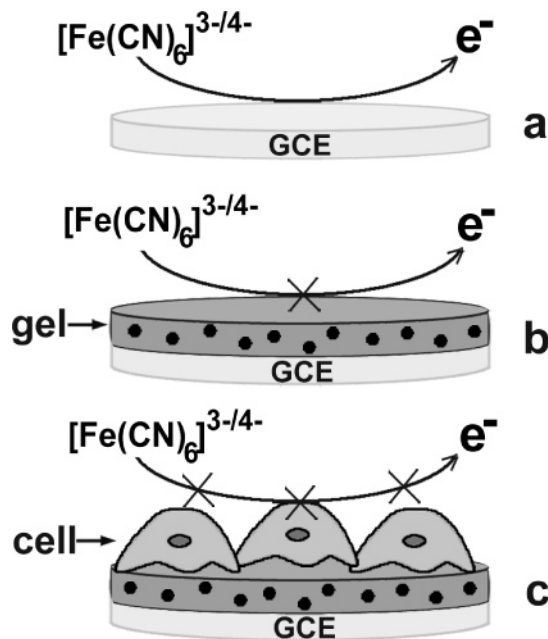


**Figure 5.** Nyquist diagrams of electrochemical impedance spectra of bare GCE (a), GNPs-CHIT gel/GCE (b), and cells/GNPs-CHIT gel/GCE (c).

**Scheme 2.** Principle for Cell-Based Impedance Sensor: (a) Bare, (b) GNPs-CHIT Gel-Modified, and (c) Cells/GNPs-CHIT Gel-Modified GCE



semicircle portion at high frequencies of Nyquist diagrams on each independently fabricated electrode. The probe showed a low resistance of  $26.4 \pm 1.5 \Omega$  upon the redox process at a bare GCE (Figure 5a). As shown in Scheme 2, the assembly of a nanocomposites layer on the electrode surface generated a tightly packed film, and the coexisted chitosan acted as a barrier

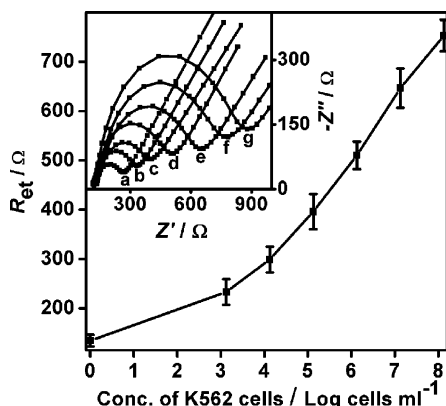


**Figure 6.** Linear relationship between electron-transfer resistance and logarithm of K562 cells concentration. Inset: Nyquist diagrams of GNPs–CHIT gel-modified GCE after immersed in (a) 0, (b)  $1.34 \times 10^3$ , (c)  $1.34 \times 10^4$ , (d)  $1.34 \times 10^5$ , (e)  $1.34 \times 10^6$ , (f)  $1.34 \times 10^7$ , and (g)  $1.34 \times 10^8$  cells  $\text{mL}^{-1}$  K562 cells suspension.

to the interfacial electron transfer, thus leading to an increase in  $R_{\text{et}}$  (Figure 5b). The  $R_{\text{et}}$  value at GNPs–CHIT gel/GCE was  $132.3 \pm 2.4 \, \Omega$ . An immobilization of the K562 cells on the gel film would further hinder the access of the redox probe to the electrode, due to the resistance of the cell membrane,<sup>25</sup> causing a further increase in  $R_{\text{et}}$  to  $610.0 \pm 5.4 \, \Omega$  (Figure 5c). The magnitude of the increase in  $R_{\text{et}}$  was related to the number of cells immobilized on the electrode surface.

**Detection of K562 Cells.** With the increasing concentration of cells in the K562 cells suspension used for immersion of the GNPs–CHIT gel/GCE, the obtained cells/GNPs–CHIT gel/GCE showed increasing diameter of the semicircle on the Nyquist diagram (inset, Figure 6), implying a higher amount of K562 cells immobilized to the electrode. A linear relationship between the  $R_{\text{et}}$  and logarithmic value of K562 cells concentration was found over a range of  $1.34 \times 10^4$  to  $1.34 \times 10^8$  cells  $\text{mL}^{-1}$  with a correlation coefficient of 0.9986 (Figure 6,  $n = 3$ ). The limit of detection calculated from the slope of the linear plot and the 10 times value of standard deviation was  $8.71 \times 10^2$  cells  $\text{mL}^{-1}$ . This detection range was wider than those of  $4.36 \times 10^5$  to  $4.36 \times 10^8$  cfu  $\text{mL}^{-1}$  for impedance immunosensor<sup>22</sup> and up to  $10^6$  cfu  $\text{mL}^{-1}$  for SPR immunosensors.<sup>34</sup> The proposed method was also more sensitive than these sensors. Because of the broad detection range, low detection limit, and simple fabrication process associated with our cell-based biosensor, it is well suited for detection of tumor cells.

**Monitoring of Cell Proliferation and Apoptosis on Electrode Surface.** The electron-transfer resistance was related to not only the amount of cells immobilized on GNPs–CHIT gel/GCE but also the proliferation and apoptosis of the adhered cells. Thus, besides the detection of cell immobilization, this method could be employed to monitor both proliferation and apoptosis of cells on electrode surface. As seen from Figure 7A, K562 cells were capable of not only adhering to GNPs–CHIT gel film but also proliferating on the film upon extended culture. With an increasing incubation time, the density of cells adhered on the film increased. After incubation for 72 h, K562 cells apparently spread evenly over the entire surface (photo c, Figure 7A). The cells were alive, as evidenced by the morphology of the distinguishable filopodia, a good indicator of cell adhesion to material surfaces and cell viability.<sup>35</sup> A longer incubation time caused the loss of cell normal characteristics and viability, presenting an abnormal morphology on the film (photo d, Figure 7A). These observations could be monitored with impedance measurements. With an increasing incubation

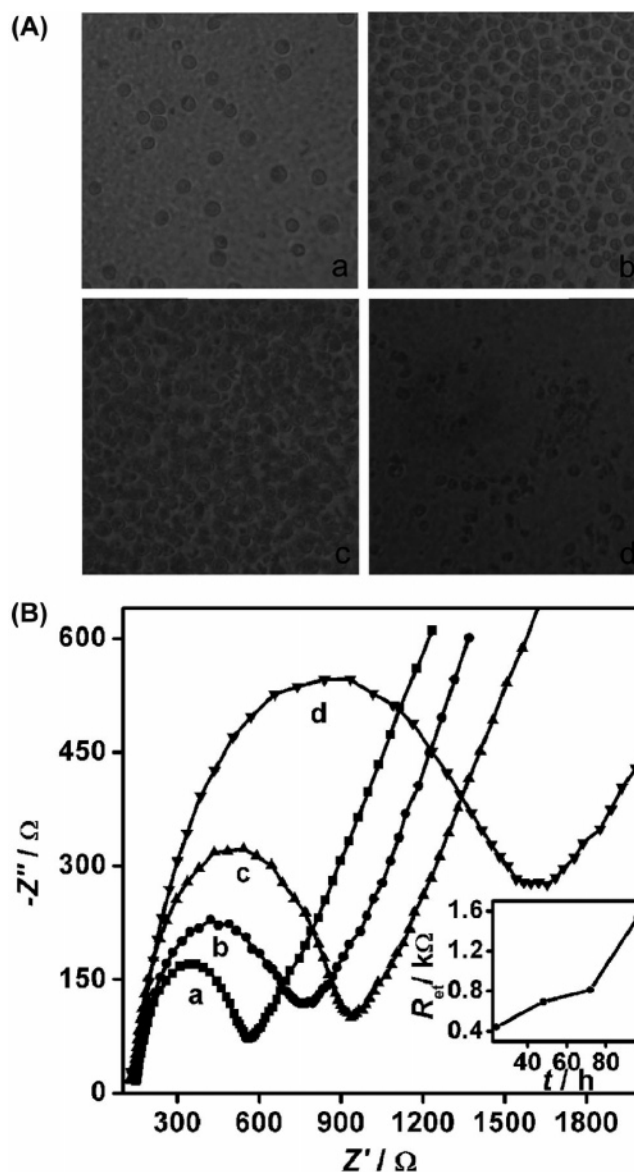


**Figure 7.** Photos of K562 cells proliferated on GNPs–CHIT gel film coated on glassy dishes at (a) 24 h, (b) 48 h, (c) 72 h, and (d) 96 h (A), and EIS measurements of K562 cells proliferated on GNPs–CHIT gel/GCE after cell incubation for (a) 24 h, (b) 48 h, (c) 72 h, and (d) 96 h (B). Inset in (B): relationship between electron-transfer resistance and proliferation time of K562 cells on GNPs–CHIT gel/GCE.

time of cells/GNPs–CHIT gel/GCE,  $R_{\text{et}}$  increased (curves a–c, Figure 7B), resulting from the cell proliferation on the electrode, which introduced a barrier for electrochemical process. The inset in Figure 7B indicates that the  $R_{\text{et}}$  of the probe increased gradually up to the incubation time of 50 h and then tended to a relatively steady value during the incubation time of 50–70 h. After the incubation time of 70 h, drastically increased resistance was observed (curve d, Figure 7B). This change might be related to the apoptosis of cells, which were congregated on the electrode surface.<sup>36</sup> These results were consistent with the observation from optical microscopy.

## Conclusions

A designer GNPs–CHIT nanocomposites gel shows excellent biocompatible spatial structure and nontoxic support for immobilization of cells, construction of cell-based sensors, and

electrochemical study of cells on surface. The support can be simply and reproducibly prepared with low cost and possesses the advantageous properties of both chitosan gel and GNPs. The cell-based impedance sensor shows a wide linear range for sensitive quantification of cells. With EIS measurements, the proposed gel film can be used for monitoring efficiently cell proliferation and apoptosis on the film. This technique provides a new avenue for electrochemical study and detection of other tumor cells by modification of electrode with the designer nanocomposites.

**Acknowledgment.** We thank the National Science Funds for Distinguished Young Scholars (20325518) and Creative Research Groups (20521503), the Key Program (20535010) from the National Natural Science Foundation of China, and the Science Foundation of Jiangsu (BS2006006, BS2006074) for financial support of this research.

## References and Notes

- (1) Du, D.; Liu, S.; Chen, J.; Ju, H.; Lian, H.; Li, J. *Biomaterials* **2005**, *26*, 6487.
- (2) Giaever, I.; Keese, C. R. *Nature* **1993**, *366*, 591.
- (3) Chen, J.; Du, D.; Yan, F.; Ju, H. X.; Lian, H. Z. *Chem.-Eur. J.* **2005**, *11*, 1467.
- (4) Daniel, M.-C.; Astruc, D. *Chem. Rev.* **2004**, *104*, 293.
- (5) Hone, D. C.; Walker, P. I.; Evans-Gowing, R.; Fitzgerald, S.; Beeby, A.; Chambrier, I.; Cook, M. J.; Russell, D. A. *Langmuir* **2002**, *18*, 2985.
- (6) Cao, Y. W. C.; Jin, R.; Mirkin, C. A. *Science* **2002**, *297*, 1536.
- (7) Corbierre, M. K.; Cameron, N. S.; Sutton, M.; Mochrie, S. G. J.; Lurio, L. B.; Rühm, A.; Lennox, R. B. *J. Am. Chem. Soc.* **2001**, *123*, 10411.
- (8) Tan, W. B.; Zhang, Y. J. *Biomed. Mater. Res.* **2005**, *75A*, 56.
- (9) Krajewska, B. *Sep. Purif. Technol.* **2005**, *41*, 305.
- (10) Betigeri, S. S.; Neau, S. H. *Biomaterials* **2002**, *23*, 3627.
- (11) Du, D.; Ju, H.; Zhang, X.; Chen, J.; Cai, J.; Chen, H. *Biochemistry* **2005**, *44*, 11539.
- (12) Yang, M. H.; Yang, Y.; Yang, H. F.; Shen, G. L.; Yu, R. Q. *Biomaterials* **2006**, *27*, 246.
- (13) Zhang, M. G.; Smith, A.; Gorski, W. *Anal. Chem.* **2004**, *76*, 5045.
- (14) Wei, X.; Zhang, M.; Gorski, W. *Anal. Chem.* **2003**, *75*, 2060.
- (15) Lu, X. B.; Ju, J. Q.; Yao, X.; Wang, Z. P.; Li, J. H. *Biomacromolecules* **2006**, *7*, 975.
- (16) Huang, H. Z.; Yang, X. R. *Biomacromolecules* **2004**, *5*, 2340.
- (17) dos Santos, D. S., Jr.; Goulet, P. J. G.; Pieczonka, N. P. W.; Oliveira, O. N., Jr.; Aroca, R. F. *Langmuir* **2004**, *20*, 10273.
- (18) Huang, H. Z.; Yuan, Q.; Yang, X. R. *J. Colloid Interface Sci.* **2005**, *282*, 26.
- (19) Anastas, P. T.; Warner, J. C. *Green Chemistry: Theory and Practice*; Oxford University Press: New York, 1998.
- (20) Park, S. M.; Yoo, J. S. *Anal. Chem.* **2003**, *75*, 455A.
- (21) Wegener, J.; Zink, S.; Rösen, P.; Galla, H.-J. *Pfluegers Arch.-Eur. J. Physiol.* **1999**, *437*, 925.
- (22) Yang, L. J.; Li, Y. B.; Erf, G. F. *Anal. Chem.* **2004**, *76*, 1107.
- (23) Ruan, C. M.; Yang, L. J.; Li, Y. B. *Anal. Chem.* **2002**, *74*, 4814.
- (24) Yang, L.; Li, Y.; Griffis, C. L.; Johnson, M. G. *Biosens. Bioelectron.* **2004**, *19*, 1139.
- (25) Chen, H.; Heng, C. K.; Pui, P. D.; Zhou, X. D.; Lee, A. C.; Lim, T. M.; Tan, S. N. *Anal. Chim. Acta* **2005**, *554*, 52.
- (26) Huang, H. Z.; Yang, X. R. *Colloids Surf., A* **2003**, *226*, 77.
- (27) Chen, J.; Yan, F.; Du, D.; Wu, J.; Ju, H. X. *Electroanalysis* **2006**, *18*, 670.
- (28) Montebault, A.; Viton, C.; Domard, A. *Biomacromolecules* **2005**, *6*, 653.
- (29) Lin, Y. H.; Chung, C. K.; Chen, C. T.; Liang, H. F.; Chen, S. C.; Sung, H. W. *Biomacromolecules* **2005**, *6*, 1104.
- (30) Liao, J. D.; Lin, S. P.; Wu, Y. T. *Biomacromolecules* **2005**, *6*, 392.
- (31) Lind, R.; Connolly, P.; Wilkinson, C. D. W.; Breckenridge, L. J.; Dow, J. A. T. *Biosens. Bioelectron.* **1991**, *6*, 359.
- (32) Bery, M. N.; Grivell, M. B. An electrochemical description of metabolism. In *Bioelectrochemistry of cells and tissues*; Walz, D., Berry, H., Milazzo, G., Eds.; Verlag: Birkhauser, Basel, 1995; p 134.
- (33) Nonner, W.; Eisenberg, B. *J. Mol. Liq.* **2000**, *87*, 149.
- (34) Koubova, V.; Brynda, E.; Karasove, L.; Skvor, J.; Homola, J.; Dostalek, J.; Tobiska, P.; Rosicky, J. *Sens. Actuators, B* **2001**, *74*, 100.
- (35) Huang, H. H. *Biochem. Biophys. Res. Commun.* **2004**, *214*, 787.
- (36) Du, D.; Cai, J.; Ju, H.; Yan, F.; Chen, J.; Jiang, X.; Chen, H. *Langmuir* **2005**, *21*, 8394.

BM061224Y